



HAL
open science

Compact explicit matrix representations of the flexoelectric tensor and a graphic method for identifying all of its rotation and reflection symmetries

H. Le Quang, Q.-C. He

► **To cite this version:**

H. Le Quang, Q.-C. He. Compact explicit matrix representations of the flexoelectric tensor and a graphic method for identifying all of its rotation and reflection symmetries. *Journal of Applied Physics*, 2021, 129 (24), pp.244103. 10.1063/5.0048386 . hal-03267829

HAL Id: hal-03267829

<https://hal.science/hal-03267829>

Submitted on 22 Jun 2021

HAL is a multi-disciplinary open access archive for the deposit and dissemination of scientific research documents, whether they are published or not. The documents may come from teaching and research institutions in France or abroad, or from public or private research centers.

L'archive ouverte pluridisciplinaire **HAL**, est destinée au dépôt et à la diffusion de documents scientifiques de niveau recherche, publiés ou non, émanant des établissements d'enseignement et de recherche français ou étrangers, des laboratoires publics ou privés.

Compact explicit matrix representations of the flexoelectric tensor and a graphic method for identifying all of its rotation and reflection symmetries

H. Le Quang^{1, a)} and Q.-C. He^{1, 2}

¹⁾ *Université Gustave Eiffel, CNRS, MSME UMR 8208, F-77454 Marne-la-Vallée, France.*

²⁾ *Southwest Jiaotong University, School of Mechanical Engineering, Chengdu 610031, PR China.*

(Dated: 17 May 2021)

Flexoelectricity is an electromechanical phenomenon produced in a dielectric material, with or without centrosymmetric microstructure, undergoing a non-uniform strain. It is characterized by the fourth-order flexoelectric tensor which links the electric polarization vector with the gradient of the second-order strain tensor. Our previous work [Le Quang and He, Roy. Soc. London, Ser. A 467, 2369-2386, 2011] solved the fundamental theoretical problem of determining the number and types of all rotational symmetries that the flexoelectric tensor can exhibit. In the present one, compact explicit matrix representations of the flexoelectric tensor are provided so as to facilitate the use of it with any possible rotational symmetry. The number and types of all reflection symmetries that the flexoelectric tensor can have are also determined. To identify the rotational symmetry and reflection symmetry of a given flexoelectric tensor, a simple and efficient graphic method based on the concept of pole figures is presented and illustrated.

PACS numbers: Valid PACS appear here

I. INTRODUCTION

Flexoelectricity is a coupled electromechanical phenomenon appearing a dielectric material subjected to a non-uniform strain. In contrast to piezoelectricity, it can be generated even in a dielectric material whose microstructure is centrosymmetric. Indeed, in the case of a dielectric material undergoing a uniform strain, the electric polarization is produced if and only if the microstructure of this material is non-centrosymmetric. However, when a dielectric material with (or without) a centrosymmetric microstructure is subjected to a non-uniform strain whose gradient is non null, a relative displacement of the centers of the positive and negative charges is resulted in and gives rise to an electric polarization.

The flexoelectric effects can be produced in a multitude of situations, for example, in bending crystal plates¹, nanobeams and nanowires²⁻⁴ or when stretching thin films⁵ on liquid crystals⁶ and on elastomers⁷. The flexoelectric constants describing the flexoelectric effects of some dielectric materials were observed and measured in a direct or indirect way in a few experimental works such as those made by Ma and Cross⁸⁻¹⁰ and Zubko *et al.*¹¹ for various perovskites which exhibit unusually high flexoelectricity, the ones of Kalinin and Meunier¹² and Naumov *et al.*¹³ for low-dimensional structures like nanographitic systems and two-dimensional boron-nitride sheets or by Zhang *et al.*^{14,15}, Chu and Salem¹⁶ and Zhou *et al.*¹⁷ for dielectric materials and polymers

such as TiO₂ ceramics and the polyvinylidene fluoride (PVDF). In parallel with these experimental works, theoretical studies were also conducted to demonstrate the size-dependent flexoelectric properties and surface effect of dielectric materials/structures in nanoscale, for example, by Sahin and Dost¹⁸, Tagantsev^{19,20}, Yurkov and Tagantsev²¹, He *et al.*²², Qi *et al.*²³ and Bai *et al.*²⁴. Numerical approaches were elaborated according either to the first-principles method, for example, by Maranganti and Sharma²⁵, Hong *et al.*^{26,27} or to the other theoretical calculation methods such as finite element method by Deng *et al.*²⁸ and Yvonnet *et al.*²⁹, phase-field method by Li *et al.*³⁰ and Wang *et al.*³¹ to estimate the flexoelectric properties of some dielectric materials/structures. For more references about flexoelectricity and for discussions on potential important applications of flexoelectricity, the reader is referred to Tagantsev *et al.*²⁰, Sharma *et al.*³², Zubko *et al.*³³, Wang *et al.*³⁴, Narvaez *et al.*³⁵, Abdollahi *et al.*³⁶ and Shu *et al.*^{37,38}.

When a dielectric material is subjected to small deformations and when the piezoelectric and flexoelectric phenomena produced in it are linear, the electric polarization vector \mathbf{p} is related to the infinitesimal strain tensor $\boldsymbol{\varepsilon}$ and the gradient of the latter, namely $\mathbb{E} = \nabla\boldsymbol{\varepsilon}$, by a linear relation:

$$p_i = D_{ijk}\varepsilon_{jk} + F_{ijkl}E_{jkl}. \quad (1)$$

Above, D_{ijk} are the matrix components of the third-order piezoelectric tensor \mathbb{D} and F_{ijkl} stand for the matrix components of the fourth-order flexoelectric tensor \mathbb{F} . Due to the symmetry $\varepsilon_{ij} = \varepsilon_{ji}$ of $\boldsymbol{\varepsilon}$, the strain gradient \mathbb{E} possesses the property $E_{ijk} = E_{jik}$ and the matrix components of \mathbb{F} have the following index permutation symmetry:

$$F_{ijkl} = F_{ikjl}. \quad (2)$$

^{a)}Corresponding author

Tel: 33 (0) 160 957 797; Fax: 33 (0) 160 957 799;
Email: hung.le-quang@univ-eiffel.fr

Note that, if the microstructure of the dielectric material in question exhibits centrosymmetry, the requirement that the third-order tensor \mathbb{D} be invariant under the central inversion transformation implies that \mathbb{D} is null, so that the constitutive law (1) reduces to

$$p_i = F_{ijkl} E_{jkl}. \quad (3)$$

In other words, when the dielectric material has a centrosymmetric microstructure, the piezoelectric effect disappears and the electric polarization vector \mathbf{p} depends only on the strain gradient \mathbb{E} .

In the linear constitutive law (1), the classical third-order piezoelectric tensor \mathbb{D} has been completely investigated and understood; however, the fourth-order flexoelectric tensor \mathbb{F} , which is much more complicated than the usual fourth-order elastic tensor, is far from being thoroughly studied and understood. In our previous one³⁹, the number and types of all possible rotational symmetries for the flexoelectric tensor \mathbb{F} were specified and the number of independent material parameters of \mathbb{F} belonging to each possible symmetry class was determined. Later, Shu *et al.*⁴⁰ gave the matrix representations of \mathbb{F} for various symmetries.

The present work can be regarded as a continuation of our previous one³⁹. Precisely, novel 3×18 matrix representations of the flexoelectric tensor \mathbb{F} are provided for all 12 rotational symmetries determined in our previous study³⁹. The matrix representations of \mathbb{F} given in the present work are well-structured and much more compact than those of Shu *et al.*⁴⁰. This should facilitate the practical use of \mathbb{F} in various anisotropic cases. In addition, the flexoelectric tensor \mathbb{F} is further investigated in the present work by determining all of its reflection symmetries. It is proved that the 12 rotational symmetry classes of the flexoelectric tensor \mathbb{F} are reduced to 8 reflection symmetries and these 8 reflection symmetries are identical to those of the fourth-order elastic tensor. Finally, a simple but efficient graphic method based on the notion of pole figures is suggested and illustrated for identifying the reflection symmetry and rotational symmetry that a given flexoelectric tensor may have.

The paper is structured as follows. In Section II, some notations and definitions used throughout the paper are presented. In Section III, the main results obtained in our previous work³⁹ on the symmetry groups and symmetry classes of the flexoelectric tensor are recalled for the paper to be self-contained. In Section IV, compact explicit matrix representations of the flexoelectric tensor for all possible rotational symmetries are provided. Section V is dedicated to finding out the reflection symmetry classes of the flexoelectric tensor. In Section VI, a simple and efficient graphic method is elaborated to identify not only the reflection symmetry but also the rotational symmetry of a given flexoelectric tensor. In Section VII,

some concluding remarks are given.

II. NOTATIONS AND DEFINITIONS

Let \mathcal{V} be a three-dimensional (3D) inner-product space over the reals \mathcal{R} and Lin be the space of all linear transformations (second-order tensors) on \mathcal{V} . The inner product of two vectors \mathbf{a} and \mathbf{b} of \mathcal{V} is symbolized by $\mathbf{a} \cdot \mathbf{b}$. The 3D orthogonal group $O(3)$ is defined as $O(3) = \{\mathbf{Q} \in Lin \mid \mathbf{Q}\mathbf{a} \cdot \mathbf{Q}\mathbf{b} = \mathbf{a} \cdot \mathbf{b}, \forall \mathbf{a}, \mathbf{b} \in \mathcal{V}\}$. The 3D rotation group $SO(3)$ is given by $SO(3) = \{\mathbf{Q} \in O(3) \mid \det \mathbf{Q} = 1\}$. In what follows, $\mathbf{Q}(\mathbf{a}, \theta)$ stands for the rotation about $\mathbf{a} \in \mathcal{V}$ through an angle $\theta \in [0, 2\pi)$. In particular, $\tilde{\mathbf{Q}}$, $\hat{\mathbf{Q}}$ and $\check{\mathbf{Q}}$ denote, respectively, the rotations $\mathbf{Q}(\mathbf{e}_1 + \mathbf{e}_2 + \mathbf{e}_3, 2\pi/3)$, $\mathbf{Q}(2\mathbf{e}_2 + \varphi^2\mathbf{e}_3, 2\pi/3)$ and $\mathbf{Q}(\varphi\mathbf{e}_2 + \mathbf{e}_3, \pi)$ with the golden ratio $\varphi = (1 + \sqrt{5})/2$.

For later use, it is convenient to introduce the following standard group notations:

(i) the identity group, denoted by I , is formed by the second-order identity tensor \mathbf{I} ;

(ii) the cyclic group Z_r ($r \geq 2$) contains r elements generated by $\mathbf{Q}(\mathbf{e}_3, 2\pi/r)$. In particular, when $r \rightarrow \infty$, Z_r becomes the group $SO(2)$ consisting of all rotations \mathbf{Q} about \mathbf{e}_3 such that $\mathbf{Q}\mathbf{e}_3 = \mathbf{e}_3$;

(iii) the dihedral group D_r ($r \geq 2$) comprises $2r$ elements generated by $\mathbf{Q}(\mathbf{e}_3, 2\pi/r)$ and $\mathbf{Q}(\mathbf{e}_1, \pi)$. The corresponding form of D_r when $r \rightarrow \infty$ is $O(2)$ consisting of all orthogonal tensors \mathbf{Q} such that $\mathbf{Q}\mathbf{e}_3 = \pm\mathbf{e}_3$;

(iv) the spatial groups \mathcal{T} , \mathcal{O} and \mathcal{I} with \mathcal{T} representing the tetrahedral group of 12 elements generated by D_2 and $\tilde{\mathbf{Q}}$, \mathcal{O} being the octahedral group of 24 elements generated by D_4 and $\hat{\mathbf{Q}}$, and \mathcal{I} symbolizing the dodecahedral group of 60 elements generated by D_5 , $\hat{\mathbf{Q}}$ and $\check{\mathbf{Q}}$. Recall that the spatial groups \mathcal{T} , \mathcal{O} and \mathcal{I} map a tetrahedron, a cube and a dodecahedron onto themselves, respectively.

Next, we define the space of flexoelectricity tensors as follows:

$$\mathcal{F} = \{\mathbb{F} = F_{ijkl}\mathbf{e}_i \otimes \mathbf{e}_j \otimes \mathbf{e}_k \otimes \mathbf{e}_l \mid F_{ijkl} = F_{ikjl}\}.$$

The symmetry group of a flexoelectricity tensor $\mathbb{F} \in \mathcal{F}$, is denoted by $\mathcal{G}(\mathbb{F})$ and characterized as

$$\mathcal{G}(\mathbb{F}) = \{\mathbf{Q} \in SO(3) \mid \mathbf{Q} * \mathbb{F} = \mathbb{F}\} \quad (4)$$

where $\mathbf{Q} * \mathbb{F} = Q_{ir}Q_{jm}Q_{kn}Q_{ls}F_{rmns}\mathbf{e}_i \otimes \mathbf{e}_j \otimes \mathbf{e}_k \otimes \mathbf{e}_l$. The definition of $\mathcal{G}(\mathbb{F})$ implies that $\mathcal{G}(\mathbb{F})$ is a closed subgroup of $SO(3)$ and $\mathcal{G}(\mathbf{Q} * \mathbb{F}) = \mathbf{Q}\mathcal{G}(\mathbb{F})\mathbf{Q}^T$ for any orthogonal tensor $\mathbf{Q} \in O(3)$. On the other hand, \mathbb{F} is said to exhibit G -symmetry when $G \subseteq \mathcal{G}(\mathbb{F})$ and $\mathbf{Q} * \mathbb{F} = \mathbb{F}$ for all $\mathbf{Q} \in G$. Consequently, two materials characterized by their respective flexoelectric tensors $\mathbb{F}_1 \in \mathcal{F}$ and $\mathbb{F}_2 \in \mathcal{F}$ are said to have the same type of symmetry if and only if the symmetry groups of \mathbb{F}_1 and \mathbb{F}_2 are conjugate to each other, i.e.

$$\mathbb{F}_1 \sim \mathbb{F}_2 \Leftrightarrow \mathcal{G}(\mathbb{F}_1) \sim \mathcal{G}(\mathbb{F}_2) \Leftrightarrow \exists \mathbf{Q} \in SO(3) \text{ such that } \mathcal{G}(\mathbb{F}_1) = \mathbf{Q}\mathcal{G}(\mathbb{F}_2)\mathbf{Q}^T. \quad (5)$$

TABLE I. List of notations

Notations	Descriptions
\mathbf{p}, p_i	Electric polarization vector and its components
\mathbb{F}, F_{ijkl}	Fourth-order (type-II) flexoelectric tensor and its components
$\tilde{\mathbf{F}}, \tilde{F}_{i\alpha}$	Matrix representation of the flexoelectric tensor and its components
\mathbb{F}^I, F_{ijkl}^I	Fourth-order type-I flexoelectric tensor and its components
\mathbb{D}, D_{ijk}	Third-order piezoelectric tensor and its components
$\boldsymbol{\varepsilon}, \varepsilon_{ij}$	Infinitesimal strain tensor and its components
\mathbb{E}, E_{ijk}	Strain gradient tensor and its components
$\tilde{\mathbf{E}}, \tilde{E}_\alpha$	Vector representation of the strain-gradient tensor and its components
$\mathbf{H}, \mathbb{H}, \mathbb{H}$	Second-, third-, fourth-order harmonic tensors
\mathcal{F}	Space of flexoelectricity tensors
\mathbf{Q}	Generic orthogonal tensor
$\mathbf{Q}(\mathbf{a}, \theta)$	Rotation about \mathbf{a} through an angle θ
$\mathcal{G}(\mathbb{F})$	Rotation symmetry group of \mathbb{F}
$\{\mathcal{G}_i\}$	Rotation symmetry class
Z_n ($n \geq 2$)	Cyclic group of order n , generated by the n -fold rotation $\mathbf{Q}(\mathbf{e}_3, \theta = 2\pi/n)$
D_n ($n \geq 2$)	Dihedral group of order $2n$ generated by Z_n and $\mathbf{Q}(\mathbf{e}_1, \pi)$
$SO(3)$	Tridimensional rotational group
$O(3)$	Tridimensional orthogonal group
\mathcal{T}	Tetrahedral group of 12 elements generated by $\mathbf{Q}(\mathbf{e}_3, \pi)$, $\mathbf{Q}(\mathbf{e}_1, \pi)$, $\mathbf{Q}(\mathbf{v}, 2\pi/3)$ with $\mathbf{v} = \frac{\sqrt{3}}{3}(\mathbf{e}_1 + \mathbf{e}_2 + \mathbf{e}_3)$
\mathcal{O}	Octahedral group of 24 elements generated by $\mathbf{Q}(\mathbf{e}_3, \pi/2)$, $\mathbf{Q}(\mathbf{e}_1, \pi)$, $\mathbf{Q}(\mathbf{v}, 2\pi/3)$ with $\mathbf{v} = \frac{\sqrt{3}}{3}(\mathbf{e}_1 + \mathbf{e}_2 + \mathbf{e}_3)$
\mathcal{I}	Dodecahedron group of 60 elements generated by $\mathbf{Q}(\mathbf{e}_3, 2\pi/5)$, $\mathbf{Q}(\mathbf{e}_1, \pi)$, $\mathbf{Q}(\mathbf{w}, 2\pi/3)$ with $\mathbf{w} = \frac{1}{\sqrt{4+\phi^2}}(2\mathbf{e}_2 + \phi\mathbf{e}_3)$ and $\phi = \frac{\sqrt{5}+1}{2}$
$SO(2)$	Subgroup of rotations $\mathbf{Q}(\mathbf{e}_3, \theta)$ with $\theta \in [0; 2\pi)$
$O(2)$	Subgroup generated by $SO(2)$ and $\mathbf{Q}(\mathbf{e}_1, \pi)$
$\mathbf{P}(\mathbf{n})$	Reflection transformation through the plane of normal \mathbf{n}
$\mathbf{P}_{\mathbb{F}}$	Set of reflection symmetry elements of \mathbb{F}
$\{\mathbf{P}_{\mathbb{F}}\}$	Reflection symmetry class of \mathbb{F}
\mathcal{P}_h	Set containing one reflection $\mathbf{P}(\mathbf{e}_3)$
\mathcal{P}_{v_k} ($k \geq 1$)	Set containing k elements $\mathcal{P}_{v_k} = \{\mathbf{P}(\mathbf{r}_3(\frac{2p\pi}{k}))\}_{1 \leq p \leq k}$ with $\mathbf{r}_3(\theta) = \sin \theta \mathbf{e}_1 + \cos \theta \mathbf{e}_2$
\mathcal{P}_{hv_k} ($k \geq 1$)	Set containing k elements of \mathcal{P}_{v_k} completed by $\mathbf{P}(\mathbf{e}_3)$
$\mathcal{P}_{\mathcal{O}}$	Cubic set consisting of 9 reflections with respect to the nine planes of which the normals of 6 pass through the center of each edge of a regular cube and the normals of 3 through the center of each face of the latter
$\mathcal{P}_{\mathcal{I}}$	Icosahedral set of 15 reflections with respect to the fifteen planes whose normals pass through the center of each edge of a regular icosahedron
$\mathcal{P}_{O(3)}$	Set composed of all reflections $\mathbf{P}(\mathbf{n})$

With the above notion of conjugacy, a family of non-empty subsets, $(\mathcal{F}_i)_{1 \leq i \leq N}$, of \mathcal{F} acts as a partition of the flexoelectric tensor space \mathcal{F} in the sense that no two elements of $(\mathcal{F}_i)_{1 \leq i \leq N}$ overlap and the union of $(\mathcal{F}_i)_{1 \leq i \leq N}$ is equal to \mathcal{F} . Thus, each element \mathcal{F}_i of this partition

characterizes a *symmetry class* for flexoelectric tensors.

On the other hand, for a given flexoelectric tensor $\mathbb{F}_i \in \mathcal{F}_i$ with the symmetry group $\mathcal{G}(\mathbb{F}_i)$, the collection of all the conjugates of $\mathcal{G}(\mathbb{F}_i)$ in the set of subgroups of $SO(3)$, i.e.

$$\{\tilde{\mathcal{G}}_i\} = \{\mathcal{G}(\mathbb{F}_i)\} = \{\tilde{\mathcal{G}} \subseteq SO(3) \mid \tilde{\mathcal{G}} = \mathbf{Q}\mathcal{G}(\mathbb{F}_i)\mathbf{Q}^T, \mathbf{Q} \in SO(3)\}, \quad (6)$$

constitutes an intrinsic characterization of the type of rotational symmetries exhibited by the elements of \mathcal{F}_i . Clearly, the definition of \mathcal{F}_i through $\{\tilde{\mathcal{G}}_i\}$ is more convenient. Finally, we denote by $\{G\}$ the collection of all the conjugates of $G \in SO(3)$ in the set of subgroups of $SO(3)$ and define $\mathcal{F}(G)$ as the set

$$\mathcal{F}(G) = \{\mathbb{F} \in \mathcal{F} \mid \mathcal{G}(\mathbb{F}) \in \{G\}\}. \quad (7)$$

For the convenience of the reader, the notations used in this paper is summarized in Table I.

III. ROTATIONAL SYMMETRY CLASSES OF THE FLEXOELECTRIC TENSOR

For the paper to be self-contained and for later use, the present section recalls the main results of our previous study³⁹ concerning the determination of the number and types of all the rotational symmetries for the flexoelectric

tensor. First, using a general method due to Spencer⁴¹, any fourth-order flexoelectric tensor $\mathbb{F} \in \mathcal{F}$ can be first decomposed into totally symmetric tensors and then split into harmonic tensors. The following explicit harmonic decomposition is established for the flexoelectric tensor \mathbb{F} :

$$\begin{aligned}
F_{ijkl} = & [\mathbb{H}]_{ijkl} \\
& + \frac{1}{3}(\epsilon_{ijm}[\mathbf{H}^{(1)}]_{klm} + \epsilon_{jkm}[\mathbf{H}^{(1)}]_{ilm} + \epsilon_{ikm}[\mathbf{H}^{(1)}]_{jlm}) + \frac{1}{4}(\epsilon_{ilm}[\mathbf{H}^{(2)}]_{jkm} + \epsilon_{jlm}[\mathbf{H}^{(2)}]_{ikm} + \epsilon_{klm}[\mathbf{H}^{(2)}]_{ijm}) \\
& + \frac{1}{7}(\delta_{ij}[\mathbf{H}^{(1)}]_{kl} + \delta_{ik}[\mathbf{H}^{(1)}]_{jl} + \delta_{il}[\mathbf{H}^{(1)}]_{jk} + \delta_{jk}[\mathbf{H}^{(1)}]_{il} + \delta_{jl}[\mathbf{H}^{(1)}]_{ik} + \delta_{kl}[\mathbf{H}^{(1)}]_{ij}) \\
& + \frac{1}{6}(3\epsilon_{ijm}\epsilon_{klm} + \epsilon_{ikm}\epsilon_{jlm} + \epsilon_{jkm}\epsilon_{ilm})[\mathbf{H}^{(2)}]_{mn} \\
& + \frac{2}{9}(2\delta_{jk}[\mathbf{H}^{(3)}]_{il} - \delta_{ik}[\mathbf{H}^{(3)}]_{jl} + \delta_{jl}[\mathbf{H}^{(3)}]_{ik} - 2\delta_{il}[\mathbf{H}^{(3)}]_{jk} + \delta_{lk}[\mathbf{H}^{(3)}]_{ji} - \delta_{ij}[\mathbf{H}^{(3)}]_{kl}) \\
& + \frac{1}{6}(\delta_{jl}[\mathbf{H}^{(4)}]_{ik} + \delta_{kl}[\mathbf{H}^{(4)}]_{ij} + \delta_{il}[\mathbf{H}^{(4)}]_{jk} - \delta_{ij}[\mathbf{H}^{(4)}]_{kl} - \delta_{ik}[\mathbf{H}^{(4)}]_{jl} - \delta_{jk}[\mathbf{H}^{(4)}]_{il}) \\
& + \frac{3}{10}(\delta_{ij}\epsilon_{klm} + \delta_{jk}\epsilon_{ilm} + \delta_{ik}\epsilon_{jlm})[\mathbf{a}^{(1)}]_m \\
& + \frac{1}{12}(2\epsilon_{kli}[\mathbf{a}^{(2)}]_j - \epsilon_{klj}[\mathbf{a}^{(2)}]_i) + \frac{1}{12}(2\epsilon_{kim}\delta_{jl} + 2\epsilon_{lim}\delta_{jk} - \epsilon_{ljm}\delta_{ik} - \epsilon_{kjm}\delta_{il} - \epsilon_{lkm}\delta_{ij})[\mathbf{a}^{(2)}]_m \\
& + \frac{1}{15}(11\epsilon_{ikm}\delta_{jl} - 4\epsilon_{jkm}\delta_{il} - 5\epsilon_{jlm}\delta_{ik} + 10\epsilon_{ilm}\delta_{jk} - 5\epsilon_{klm}\delta_{ij} + 3\epsilon_{ijm}\delta_{kl})[\mathbf{a}^{(3)}]_m \\
& + \frac{1}{15}(3\epsilon_{ijk}[\mathbf{a}^{(3)}]_l + 3\epsilon_{ijl}[\mathbf{a}^{(3)}]_k + \epsilon_{ikl}[\mathbf{a}^{(3)}]_j + \epsilon_{jkl}[\mathbf{a}^{(3)}]_i) \\
& + \frac{\alpha_1}{15}(\delta_{ij}\delta_{kl} + \delta_{ik}\delta_{jl} + \delta_{il}\delta_{jk}) + \frac{\alpha_2}{3}(\delta_{jl}\delta_{ik} + \delta_{ij}\delta_{kl} - 2\delta_{il}\delta_{jk}). \tag{8}
\end{aligned}$$

It can be seen from (8) that the harmonic decomposition of \mathbb{F} contains : two scalars α_1 and α_2 ; three vectors $\mathbf{a}^{(1)}$, $\mathbf{a}^{(2)}$ and $\mathbf{a}^{(3)}$; four second-order harmonic tensors $\mathbf{H}^{(1)}$, $\mathbf{H}^{(2)}$, $\mathbf{H}^{(3)}$ and $\mathbf{H}^{(4)}$; two third-order harmonic tensors

$\mathbb{H}^{(1)}$ and $\mathbb{H}^{(2)}$ and a fourth-order harmonic tensor \mathbb{H} . The components of these harmonic tensors are explicitly expressed in terms of F_{ijkl} as

$$\alpha_1 = \frac{1}{3}(F_{ppqq} + 2F_{ppqq}), \quad \alpha_2 = \frac{1}{3}\epsilon_{pqk}\epsilon_{mnk}F_{(mp)nq}, \tag{9}$$

$$[\mathbf{a}^{(1)}]_k = \frac{1}{9}\epsilon_{pqk}(F_{pmmq} + 2F_{mmpq}), \quad [\mathbf{a}^{(2)}]_k = \epsilon_{mnp}F_{mnkp}, \quad [\mathbf{a}^{(3)}]_k = \frac{1}{6}(\epsilon_{pqk}F_{pqmm} + \epsilon_{pqn}F_{pqkn}), \tag{10}$$

$$\begin{aligned}
[\mathbf{H}^{(1)}]_{km} &= F_{(ppkm)} - \frac{1}{3}\alpha_1\delta_{km}, & [\mathbf{H}^{(2)}]_{km} &= \frac{1}{2}(\epsilon_{pqk}\epsilon_{lnm} + \epsilon_{pqm}\epsilon_{lnk})F_{(lp)nq} - \alpha_2\delta_{km}, \\
[\mathbf{H}^{(3)}]_{km} &= \frac{1}{2}\epsilon_{lnq}(\epsilon_{pqm}F_{(lp)nk} + \epsilon_{pqk}F_{(lp)nm}), & [\mathbf{H}^{(4)}]_{km} &= \frac{1}{2}\epsilon_{lnq}(\epsilon_{pqm}F_{(lpk)n} + \epsilon_{pqk}F_{(lpm)n}), \tag{11}
\end{aligned}$$

$$\begin{aligned}
[\mathbf{H}^{(1)}]_{kmn} &= [\mathbf{S}^{(1)}]_{(kmn)} - \frac{1}{5}(\delta_{mn}[\mathbf{a}^{(3)}]_k + \delta_{km}[\mathbf{a}^{(3)}]_n + \delta_{kn}[\mathbf{a}^{(3)}]_m), \\
[\mathbf{H}^{(2)}]_{kmn} &= [\mathbf{S}^{(2)}]_{(kmn)} - \frac{1}{5}(\delta_{mn}[\mathbf{a}^{(1)}]_k + \delta_{km}[\mathbf{a}^{(1)}]_n + \delta_{kn}[\mathbf{a}^{(1)}]_m),
\end{aligned} \tag{12}$$

$$\begin{aligned}
[\mathbb{H}]_{klmn} &= F_{(klmn)} - \frac{1}{7}(\delta_{kl}[\mathbf{H}^{(1)}]_{mn} + \delta_{km}[\mathbf{H}^{(1)}]_{ln} + \delta_{kn}[\mathbf{H}^{(1)}]_{lm} + \delta_{lm}[\mathbf{H}^{(1)}]_{kn} + \delta_{ln}[\mathbf{H}^{(1)}]_{km} + \delta_{mn}[\mathbf{H}^{(1)}]_{kl}) \\
&\quad - \frac{\alpha_1}{15}(\delta_{kl}\delta_{mn} + \delta_{km}\delta_{ln} + \delta_{kn}\delta_{lm}).
\end{aligned} \tag{13}$$

Above, δ_{ij} and ϵ_{ijk} are the Kronecker delta and permutation symbol, respectively; either $\bullet_{i_1 i_2 \dots i_n}$ or $[\bullet]_{i_1 i_2 \dots i_n}$ is the component of an n th-order tensor \bullet ; $\bullet_{(i_1 i_2 \dots i_r) i_{r+1} \dots i_n}$ denotes the average of $r!$ components obtained by permuting the indices i_1, i_2, \dots, i_r in all possible ways; the

third-order tensors \mathbb{S}_1 and \mathbb{S}_2 are defined as

$$[\mathbb{S}^{(1)}]_{kmn} = \epsilon_{pqn} F_{(pk)qm}, \quad [\mathbb{S}^{(2)}]_{kmn} = \epsilon_{pqn} F_{(pkm)q}. \tag{14}$$

Next, by using the Cartan method, the second-, third- and fourth-order harmonic tensors $\mathbf{H}^{(i)}$, $\mathbb{H}^{(i)}$ and \mathbb{H} in Eq. (8) can be rewritten as follows:

$$\begin{aligned}
\mathbf{H}^{(i)} &= \alpha_{0i}^{(2)} \mathbf{U}_0 + \alpha_{1i}^{(2)} \mathbf{U}_1 + \beta_{1i}^{(2)} \mathbf{T}_1 + \alpha_{2i}^{(2)} \mathbf{U}_2 + \beta_{2i}^{(2)} \mathbf{T}_2 \text{ with } i = 1, 2, 3, 4, \\
\mathbb{H}^{(i)} &= \alpha_{0i}^{(3)} \mathbb{U}_0 + \alpha_{1i}^{(3)} \mathbb{U}_1 + \beta_{1i}^{(3)} \mathbb{T}_1 + \alpha_{2i}^{(3)} \mathbb{U}_2 + \beta_{2i}^{(3)} \mathbb{T}_2 + \alpha_{3i}^{(3)} \mathbb{U}_3 + \beta_{3i}^{(3)} \mathbb{T}_3 \text{ with } i = 1, 2, \\
\mathbb{H} &= \alpha_0^{(4)} \mathbb{U}_0 + \alpha_1^{(4)} \mathbb{U}_1 + \beta_1^{(4)} \mathbb{T}_1 + \alpha_2^{(4)} \mathbb{U}_2 + \beta_2^{(4)} \mathbb{T}_2 + \alpha_3^{(4)} \mathbb{U}_3 + \beta_3^{(4)} \mathbb{T}_3 + \alpha_4^{(4)} \mathbb{U}_4 + \beta_4^{(4)} \mathbb{T}_4,
\end{aligned} \tag{15}$$

where \mathbf{U}_i , \mathbf{T}_i , \mathbb{U}_i , \mathbb{T}_i , \mathbb{U}_i and \mathbb{T}_i are the tensors involved in the Cartan decomposition, whose explicit expressions can be found in Forte and Vianello^{42,43} or Le Quang and He³⁹.

With the help of the harmonic and Cartan decompositions presented above, it can be shown that the number of all possible rotational symmetry classes for all flexoelectric tensors is 12. These 12 symmetry classes are characterized by the conjugates of the following 12 sub-

groups of $SO(3)$:

$$I, \{Z_r\}, \{D_r\}, \{\mathcal{O}\}, \{\mathcal{T}\}, \{SO(2)\}, \{O(2)\}, SO(3) \tag{16}$$

where $2 \leq r \leq 4$.

Alternatively, the 12 sets $\mathcal{F}(I)$, $\mathcal{F}(Z_r)$, $\mathcal{F}(D_r)$ with $2 \leq r \leq 4$, $\mathcal{F}(\mathcal{O})$, $\mathcal{F}(\mathcal{T})$, $\mathcal{F}(SO(2))$, $\mathcal{F}(O(2))$, $\mathcal{F}(SO(3))$ form a partition of the flexoelectric tensor space \mathcal{F} :

$$\mathcal{F} = \mathcal{F}(I) \cup_{r=2}^4 \mathcal{F}(Z_r) \cup_{r=2}^4 \mathcal{F}(D_r) \cup \mathcal{F}(\mathcal{O}) \cup \mathcal{F}(\mathcal{T}) \cup \mathcal{F}(SO(2)) \cup \mathcal{F}(O(2)) \cup \mathcal{F}(SO(3)). \tag{17}$$

For more detail about the derivation of these results, the reader can refer to our previous work³⁹.

IV. COMPACT EXPLICIT MATRIX REPRESENTATIONS OF THE FLEXOELECTRIC TENSOR

In order to obtain explicit matrix expressions of the fourth-order flexoelectric tensor for all the 12 rotational

symmetry classes, we first adopt the following reduced suffix notations for the gradient \mathbb{E} of the infinitesimal strain tensor $\boldsymbol{\varepsilon}$ and for the fourth-order flexoelectric tensor $\mathbb{F} \in \mathcal{F}$:

$$\tilde{E}_\gamma = \left[\sqrt{2}(1 - \delta_{jk}) + \delta_{jk} \right] E_{jkl}, \tag{18}$$

$$\tilde{F}_{i\gamma} = \left[\sqrt{2}(1 - \delta_{jk}) + \delta_{jk} \right] F_{ijkl}, \tag{19}$$

TABLE II. Suffix notation correspondences between (j, k, l) and γ .

(j, k, l) or (m, n, s)	γ or ζ
(1,1,1)	1
(2,2,1)	2
(1,2,2) or (2,1,2)	3
(3,3,1)	4
(1,3,3) or (3,1,3)	5
(2,2,2)	6
(1,1,2)	7
(1,2,1) or (2,1,1)	8
(3,3,2)	9
(2,3,3) or (3,2,3)	10
(3,3,3)	11
(1,1,3)	12
(1,3,1) or (3,1,1)	13
(2,2,3)	14
(2,3,2) or (3,2,2)	15
(1,2,3) or (2,1,3)	16
(1,3,2) or (3,1,2)	17
(2,3,1) or (3,2,1)	18

where γ defined in Table II and the summation convention does not apply on j and k .

According to the previously reduced notation rules, the constitutive relation (3) between the electric polarization and the gradient of the infinitesimal strain tensor can now be written in the following matrix form:

$$\mathbf{p} = \tilde{\mathbf{F}} \cdot \tilde{\mathbf{E}} \quad (20)$$

where the vectors \mathbf{p} and $\tilde{\mathbf{E}}$ are specified by

$$\begin{aligned} \mathbf{p} &= [p_1 \ p_2 \ p_3]^T, \\ \tilde{\mathbf{E}} &= [\tilde{E}_1 \ \tilde{E}_2 \ \dots \ \tilde{E}_{18}]^T, \end{aligned} \quad (21)$$

and $\tilde{\mathbf{F}}$ is the 3×18 flexoelectric matrix whose block matrix representation has the general expression

$$\tilde{\mathbf{F}} = \begin{bmatrix} D_x & C_{xy} & C_{xz} & J_x \\ C_{yx} & D_y & C_{yz} & J_y \\ C_{zx} & C_{zy} & D_z & J_z \end{bmatrix}.$$

Here, the diagonal block matrices D_x , D_y and D_z of D -type and extra-diagonal block matrices C_{xy} , C_{xz} , C_{yx} , C_{yz} , C_{zx} and C_{zy} of C -type have the same size 1×5 while the extra-diagonal block matrices J_x , J_y and J_z of J -type are of the size 1×3 .

With the previously reduced notation rules, the action of an orthogonal tensor $\mathbf{Q} \in O(3)$ on a flexoelectric tensor \mathbb{F} can be expressed in the following simple and explicit matrix form:

$$Q_{ir} Q_{jm} Q_{kn} Q_{ls} F_{rmns} = Q_{ir} \tilde{F}_{r\zeta} \tilde{Q}_{\zeta\gamma} \quad (22)$$

where $\tilde{Q}_{\zeta\gamma}$, standing for the components of the 18×18 matrix $\tilde{\mathbf{Q}}$, are given by

$$\begin{aligned} \tilde{Q}_{\zeta\gamma} &= \left[\sqrt{2}(1 - \delta_{jk}) + \delta_{jk} \right] \\ &\times \left[\sqrt{2}(1 - \delta_{mn}) + \delta_{mn} \right] Q_{jm} Q_{kn} Q_{ls}. \end{aligned} \quad (23)$$

Above, γ and ζ are defined in Table II and the summation convention does not hold for j, k, m and n .

By using the procedure elaborated in Le Quang and He³⁹ to construct a flexoelectric tensor \mathbb{F} exhibiting a required symmetry and by exploiting the harmonic and Cartan decompositions in Eqs. (8) and (15) together with the Cartan decomposition parameters $\alpha_{\bullet}^{(\bullet)}$ and $\beta_{\bullet}^{(\bullet)}$ provided in Table III, we can exactly calculate the number of independent components contained in a flexoelectric tensor $\mathbb{F} \in \mathcal{F}$ belonging to a given symmetry class. The corresponding results are shown in Table IV.

Next, by adopting the above reduced suffix notations for the fourth-order flexoelectric tensor \mathbb{F} , we obtain the explicit matrix forms of the elementary block matrices of (D, C, J) -type as well as the explicit matrix form of $\tilde{\mathbf{F}}$ for each symmetry class. These explicit block matrix forms of $\tilde{\mathbf{F}}$ are provided as follows:

Identity class: I

$$\tilde{\mathbf{F}}_I = \begin{bmatrix} D_x^{(5)} & C_{xy}^{(5)} & C_{xz}^{(5)} & J_x^{(3)} \\ C_{yx}^{(5)} & D_y^{(5)} & C_{yz}^{(5)} & J_y^{(3)} \\ C_{zx}^{(5)} & C_{zy}^{(5)} & D_z^{(5)} & J_z^{(3)} \end{bmatrix}, \quad (24)$$

Cyclic classes: Z_r

$$\tilde{\mathbf{F}}_{Z_2} = \begin{bmatrix} D_x^{(5)} & C_{xy}^{(5)} & 0 & 0 \\ C_{yx}^{(5)} & D_y^{(5)} & 0 & 0 \\ 0 & 0 & D_z^{(5)} & J_z^{(3)} \end{bmatrix}, \quad (25)$$

$$\tilde{\mathbf{F}}_{Z_3} = \begin{bmatrix} D^{(4)} & C_{xy}^{(4)} & C_{xz}^{(2)} & C_{yz}^{(2)} \cdot P_1 \\ -C_{xy}^{(4)} & D^{(4)} & C_{yz}^{(2)} & -C_{xz}^{(2)} \cdot P_1 \\ C_{zx}^{(1)} & C_{zy}^{(1)} & D_z^{(3)} & J_z^{(1)} \end{bmatrix}, \quad (26)$$

$$\tilde{\mathbf{F}}_{Z_4} = \begin{bmatrix} D^{(5)} & C_{xy}^{(5)} & 0 & 0 \\ -C_{xy}^{(5)} & D^{(5)} & 0 & 0 \\ 0 & 0 & D_z^{(3)} & J_z^{(1)} \end{bmatrix}, \quad (27)$$

$$\tilde{\mathbf{F}}_{SO(2)} = \begin{bmatrix} D^{(4)} & C_{xy}^{(4)} & 0 & 0 \\ -C_{xy}^{(4)} & D^{(4)} & 0 & 0 \\ 0 & 0 & D_z^{(3)} & J_z^{(1)} \end{bmatrix}, \quad (28)$$

Dihedral classes: D_r

$$\tilde{\mathbf{F}}_{D_2} = \begin{bmatrix} D_x^{(5)} & 0 & 0 & 0 \\ 0 & D_y^{(5)} & 0 & 0 \\ 0 & 0 & D_z^{(5)} & 0 \end{bmatrix}, \quad (29)$$

$$\tilde{\mathbf{F}}_{D_3} = \begin{bmatrix} D^{(4)} & 0 & 0 & C_{yz}^{(2)} \cdot P_1 \\ 0 & D^{(4)} & C_{yz}^{(2)} & 0 \\ 0 & C_{zy}^{(1)} & D_z^{(3)} & 0 \end{bmatrix}, \quad (30)$$

$$\tilde{\mathbf{F}}_{D_4} = \begin{bmatrix} D^{(5)} & 0 & 0 & 0 \\ 0 & D^{(5)} & 0 & 0 \\ 0 & 0 & D_z^{(3)} & 0 \end{bmatrix}, \quad (31)$$

$$\tilde{\mathbf{F}}_{O(2)} = \begin{bmatrix} D^{(4)} & 0 & 0 & 0 \\ 0 & D^{(4)} & 0 & 0 \\ 0 & 0 & D_z^{(3)} & 0 \end{bmatrix}, \quad (32)$$

TABLE III. Zero components \cdot and non-zero independent material parameters \bullet contained in a flexoelectric tensor belonging to a given symmetry class

Parameters	I	$\{Z_2\}$	$\{D_2\}$	$\{Z_3\}$	$\{D_3\}$	$\{Z_4\}$	$\{D_4\}$	$\{\mathcal{T}\}^a$	$\{\mathcal{O}\}^b$	$\{O(2)\}$	$\{SO(2)\}$	$\{SO(3)\}$
α_1	\bullet	\bullet	\bullet	\bullet	\bullet	\bullet	\bullet	\bullet	\bullet	\bullet	\bullet	\bullet
α_2	\bullet	\bullet	\bullet	\bullet	\bullet	\bullet	\bullet	\bullet	\bullet	\bullet	\bullet	\bullet
$a_1^{(i)}$	\bullet	\cdot	\cdot	\cdot	\cdot	\cdot	\cdot	\cdot	\cdot	\cdot	\cdot	\cdot
$a_2^{(i)}$	\bullet	\cdot	\cdot	\cdot	\cdot	\cdot	\cdot	\cdot	\cdot	\cdot	\cdot	\cdot
$a_3^{(i)}$	\bullet	\cdot	\bullet	\bullet	\cdot	\bullet	\cdot	\cdot	\cdot	\cdot	\bullet	\cdot
$\alpha_{0i}^{(2)}$	\bullet	\bullet	\bullet	\bullet	\bullet	\bullet	\bullet	\cdot	\cdot	\bullet	\bullet	\cdot
$\alpha_{1i}^{(2)}$	\bullet	\cdot	\cdot	\cdot	\cdot	\cdot	\cdot	\cdot	\cdot	\cdot	\cdot	\cdot
$\beta_{1i}^{(2)}$	\bullet	\cdot	\cdot	\cdot	\cdot	\cdot	\cdot	\cdot	\cdot	\cdot	\cdot	\cdot
$\alpha_{2i}^{(2)}$	\bullet	\bullet	\bullet	\cdot	\cdot	\cdot	\cdot	\cdot	\cdot	\cdot	\cdot	\cdot
$\beta_{2i}^{(2)}$	\bullet	\bullet	\cdot	\cdot	\cdot	\cdot	\cdot	\cdot	\cdot	\cdot	\cdot	\cdot
$\alpha_{0i}^{(3)}$	\bullet	\bullet	\cdot	\bullet	\cdot	\bullet	\cdot	\cdot	\cdot	\cdot	\bullet	\cdot
$\alpha_{1i}^{(3)}$	\bullet	\cdot	\cdot	\cdot	\cdot	\cdot	\cdot	\cdot	\cdot	\cdot	\cdot	\cdot
$\beta_{1i}^{(3)}$	\bullet	\cdot	\cdot	\cdot	\cdot	\cdot	\cdot	\cdot	\cdot	\cdot	\cdot	\cdot
$\alpha_{2i}^{(3)}$	\bullet	\bullet	\cdot	\cdot	\cdot	\cdot	\cdot	\cdot	\cdot	\cdot	\cdot	\cdot
$\beta_{2i}^{(3)}$	\bullet	\bullet	\bullet	\cdot	\cdot	\cdot	\cdot	\bullet	\cdot	\cdot	\cdot	\cdot
$\alpha_{3i}^{(3)}$	\bullet	\cdot	\cdot	\bullet	\bullet	\cdot	\cdot	\cdot	\cdot	\cdot	\cdot	\cdot
$\beta_{3i}^{(3)}$	\bullet	\cdot	\cdot	\bullet	\cdot	\cdot	\cdot	\cdot	\cdot	\cdot	\cdot	\cdot
$\alpha_0^{(4)}$	\bullet	\bullet	\bullet	\bullet	\bullet	\bullet	\bullet	\bullet	\bullet	\bullet	\bullet	\cdot
$\alpha_1^{(4)}$	\bullet	\cdot	\cdot	\cdot	\cdot	\cdot	\cdot	\cdot	\cdot	\cdot	\cdot	\cdot
$\beta_1^{(4)}$	\bullet	\cdot	\cdot	\cdot	\cdot	\cdot	\cdot	\cdot	\cdot	\cdot	\cdot	\cdot
$\alpha_2^{(4)}$	\bullet	\bullet	\bullet	\cdot	\cdot	\cdot	\cdot	\cdot	\cdot	\cdot	\cdot	\cdot
$\beta_2^{(4)}$	\bullet	\bullet	\cdot	\cdot	\cdot	\cdot	\cdot	\cdot	\cdot	\cdot	\cdot	\cdot
$\alpha_3^{(4)}$	\bullet	\cdot	\cdot	\bullet	\cdot	\cdot	\cdot	\cdot	\cdot	\cdot	\cdot	\cdot
$\beta_3^{(4)}$	\bullet	\cdot	\cdot	\bullet	\bullet	\cdot	\cdot	\cdot	\cdot	\cdot	\cdot	\cdot
$\alpha_4^{(4)}$	\bullet	\bullet	\bullet	\cdot	\cdot	\bullet	\bullet	\bullet	\bullet	\cdot	\cdot	\cdot
$\beta_4^{(4)}$	\bullet	\bullet	\cdot	\cdot	\cdot	\bullet	\cdot	\cdot	\cdot	\cdot	\cdot	\cdot

$$^a \alpha_4^{(4)} = 5\alpha_0^{(4)}$$

$$^b \alpha_4^{(4)} = 5\alpha_0^{(4)}$$

TABLE IV. Number of independent material parameters contained in a flexoelectric tensor belonging to a given symmetry class

Symmetry class	I	$\{Z_2\}$	$\{D_2\}$	$\{Z_3\}$	$\{D_3\}$	$\{Z_4\}$	$\{D_4\}$	$\{\mathcal{T}\}$	$\{\mathcal{O}\}$	$\{O(2)\}$	$\{SO(2)\}$	$\{SO(3)\}$
Number of independent components	54	28	15	18	10	14	8	5	3	7	12	2

Spatial classes:

$$\tilde{\mathbf{F}}_{\mathcal{T}} = \begin{bmatrix} D^{(5)} & 0 & 0 & 0 \\ 0 & D^{(5)} \cdot P_2 & 0 & 0 \\ 0 & 0 & D^{(5)} & 0 \end{bmatrix}, \quad (33)$$

$$\tilde{\mathbf{F}}_{\mathcal{O}} = \begin{bmatrix} D^{(3)} & 0 & 0 & 0 \\ 0 & D^{(3)} & 0 & 0 \\ 0 & 0 & D^{(3)} & 0 \end{bmatrix}, \quad (34)$$

$$\tilde{\mathbf{F}}_{SO(3)} = \begin{bmatrix} D^{(2)} & 0 & 0 & 0 \\ 0 & D^{(2)} & 0 & 0 \\ 0 & 0 & D^{(2)} & 0 \end{bmatrix}. \quad (35)$$

In Eqs. (25)-(35), the superscript of each elementary block matrix of D , C or J -type denotes the number of independent material parameters; P_1 and P_2 are two cor-

rection matrices. By introducing two material parameters defined as

$$\eta = \frac{1}{\sqrt{2}}(\tilde{F}_{11} - \tilde{F}_{12}), \quad \theta = \frac{1}{\sqrt{2}}(\tilde{F}_{22} - \tilde{F}_{21}), \quad (36)$$

the elementary block matrices of (D, C, J) -types as well as of the correction matrices P_1 and P_2 are explicitly expressed as follows:

D-type elements:

$$D^{(5)} = [d_1 \ d_2 \ d_3 \ d_4 \ d_5], \quad (37)$$

$$D^{(4)} = [d_1 \ d_2 \ \eta \ d_4 \ d_5], \quad (38)$$

$$D^{(3)} = [d_1 \ d_2 \ d_3 \ d_2 \ d_3], \quad (39)$$

$$D^{(2)} = [d_1 \ d_2 \ \eta \ d_2 \ \eta], \quad (40)$$

C-type elements:

$$C^{(5)} = [c_1 \ c_2 \ c_3 \ c_4 \ c_5], \quad (41)$$

$$C^{(4)} = [c_1 \ c_2 \ \theta \ c_4 \ c_5], \quad (42)$$

$$C^{(2)} = [0 \ c_2 \ c_3 \ -c_2 \ -c_3], \quad (43)$$

$$C^{(1)} = [c_1 \ -c_1 \ -c_1 \ 0 \ 0], \quad (44)$$

J-type elements:

$$J^{(3)} = [j_1 \ j_2 \ j_3], \quad J^{(1)} = [0 \ j_2 \ -j_2 \ \], \quad (45)$$

Correction elements:

$$P_1 = \begin{bmatrix} 0 & 0 & 0 \\ 1 & 0 & 0 \\ 0 & 1 & 1 \\ 0 & 0 & 0 \\ 0 & 0 & 1 \end{bmatrix}, P_2 = \begin{bmatrix} 1 & 0 & 0 & 0 & 0 \\ 0 & 0 & 0 & 1 & 0 \\ 0 & 0 & 0 & 0 & 1 \\ 0 & 1 & 0 & 0 & 0 \\ 0 & 0 & 1 & 0 & 0 \end{bmatrix}. \quad (46)$$

Finally, the compact explicit matrix expressions for the 12 symmetry classes of flexoelectric tensors are shown in Table V.

V. REFLECTION SYMMETRY CLASSES OF THE FLEXOELECTRIC TENSOR

First, let us introduce $\mathbf{P}(\mathbf{n}) \in \text{O}(3) \setminus \text{SO}(3)$, the reflection through the plane $\mathcal{P}(\mathbf{n}) = \{\mathbf{x} \in \mathbb{R}^3 \mid \mathbf{x} \cdot \mathbf{n} = 0\}$ perpendicular to a unit vector \mathbf{n} , by

$$\mathbf{P}(\mathbf{n}) = \mathbf{I} - 2\mathbf{n} \otimes \mathbf{n}. \quad (47)$$

It can be seen from (47) that \mathbf{P} is an even function of \mathbf{n} in the sense that $\mathbf{P}(-\mathbf{n}) = \mathbf{P}(\mathbf{n})$. Thus, two unit normal vectors are associated to each reflection.

Next, we denote by $\mathbf{P}_{\mathbb{F}}$ the set of reflection symmetry elements of $\mathbb{F} \in \mathcal{F}$. The reflection symmetry class of $\mathbb{F} \in \mathcal{F}$, symbolized by $\{\mathbf{P}_{\mathbb{F}}\}$, is defined as the collection of all the conjugates of $\mathbf{P}_{\mathbb{F}}$, namely

$$\{\mathbf{P}_{\mathbb{F}}\} = \{\mathbf{P}'_{\mathbb{F}} = \mathbf{R}\mathbf{P}_{\mathbb{F}}\mathbf{R}^T \mid \mathbf{R} \in \text{SO}(3)\}. \quad (48)$$

Note that $\{\mathbf{P}_{\mathbb{F}}\}$ represents the reflection symmetry class and not the symmetry group of $\mathbb{F} \in \mathcal{F}$.

We introduce the unit vector

$$\mathbf{r}_i(\theta) = \sin \theta \mathbf{e}_j + \cos \theta \mathbf{e}_k \quad (49)$$

with $\{i, j, k\}$ being a cycle permutation of $\{1, 2, 3\}$, and the following sets of reflection transformations:

- \mathcal{P}_h being the set which contains only the reflection $\mathbf{P}(\mathbf{e}_3)$. The label h means “horizontal”.
- \mathcal{P}_{v_k} being the set defined by $\mathcal{P}_{v_k} = \{\mathbf{P}(\mathbf{r}_3(\frac{2p\pi}{k}))\}_{1 \leq p \leq k}$ and consisting of k elements. The label v means “vertical”.
- \mathcal{P}_{hv_k} ($k \geq 1$) being the set defined by the k elements of \mathcal{P}_{v_k} completed by $\mathbf{P}(\mathbf{e}_3)$: this set comprises $k+1$ elements.

- $\mathcal{P}_{\mathcal{O}}$ designating the cubic set of nine reflections with respect to the nine planes of which the normals of 6 pass through the center of each edge of a regular cube and the normals of 3 through the center of each face of the latter.
- $\mathcal{P}_{\mathcal{I}}$ denoting the icosahedral set consisting of fifteen reflections with respect to the fifteen planes whose normals pass through the center of each edge of a regular icosahedron;
- $\mathcal{P}_{\text{O}(3)}$ representing the set composed of all reflections $\mathbf{P}(\mathbf{n})$ with $\mathbf{n} \in \mathcal{S}^2$ where \mathcal{S}^2 is the unit sphere defined by $\mathcal{S}^2 = \{\mathbf{x} \in \mathbb{R}^3 \mid \|\mathbf{x}\| = 1\}$.

We can show that the space \mathcal{F} of flexoelectric tensors is divided into the 8 reflection symmetry classes which are characterized by the following 8 sets of reflection transformations:

$$\emptyset, \{\mathcal{P}_h\}, \{\mathcal{P}_{hv_2}\}, \{\mathcal{P}_{v_3}\}, \{\mathcal{P}_{hv_4}\}, \{\mathcal{P}_{hv_\infty}\}, \{\mathcal{P}_{\mathcal{O}}\}, \{\mathcal{P}_{\text{O}(3)}\}. \quad (50)$$

The characteristics of each reflection symmetry class, and especially its link with the rotational ones, are detailed in Table VI. It is important and interesting to remark that: (i) unlike the results as obtained by Chadwick *et al.*⁴⁴ for the space of fourth-order elasticity tensors, according to which the classifications by rotational symmetry groups and by reflection symmetry planes give the same response, the number of rotational symmetry classes for the space of fourth-order flexoelectric tensors is 12 while the one of reflection symmetry classes is only 8; (ii) these 8 reflection symmetry classes for the space of flexoelectric tensors are exactly identical to the ones for the space of elasticity tensors, even through a fourth-order flexoelectric tensor is algebraically more complex than a fourth-order elasticity tensor.

VI. A GRAPHIC METHOD FOR IDENTIFYING REFLECTION AND ROTATIONAL SYMMETRIES

The important question now arises as to how to identify the reflection symmetry and rotational symmetry and of a given flexoelectric tensor from the knowledge of its matrix relative to a basis. The present section aims at elaborating a simple but efficient graphic method to answer this question.

Francois *et al.*⁴⁵ initiated a graphic approach to identifying the reflection symmetry planes that a given fourth-order elastic tensor has. This approach is based on the notion of “pole figures”. Owing to the fact that the reflection symmetry classes of the fourth-order elastic tensor are identical to its rotational symmetry classes, the identification of the formers leads also the one of the latters. However, when the fourth-order elastic tensor is concerned, the situation is much more complicated, since its reflection symmetry classes are 8 while its reflection symmetry classes are 12. Thus, in this section we extend

TABLE V. Number of independent material parameters and compact explicit matrix expression for each of the 12 symmetry classes of flexoelectric tensors

Key to notation	
• : non-zero component	●—● : equal components
· : zero component	●—○ : components numerically equal, but opposite in sign
x : $\frac{1}{\sqrt{2}}(\tilde{F}_{11} - \tilde{F}_{12})$	*—⊗ : components numerically equal, but opposite in sign
* : $\frac{1}{\sqrt{2}}(\tilde{F}_{22} - \tilde{F}_{21})$	



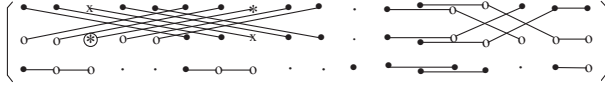





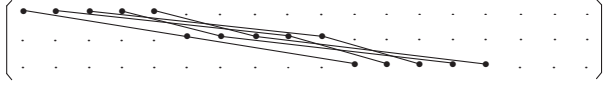


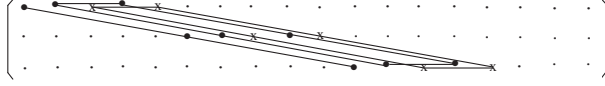
<p>Triclinic (54)</p> 	<p>Monoclinic Z_2 (28)</p> 
<p>Trigonal Z_3 (18)</p> 	<p>Orthotropic D_2 (15)</p> 
<p>Trigonal D_3 (10)</p> 	<p>Tetragonal Z_4 (14)</p> 
<p>Cubic \mathcal{O} (3)</p> 	<p>Tetragonal D_4 (8)</p> 
<p>Tetrahedral \mathcal{T} (5)</p> 	<p>Trans. Iso. $O(2)$ (7)</p> 
<p>Trans. Iso. $SO(2)$ (12)</p> 	<p>Isotropic $SO(3)$ (2)</p> 

TABLE VI. Symmetry plane stratification of the space \mathcal{F} of fourth-order flexoelectric tensors

System	Reflection symmetry class	Number of reflection symmetry planes	Rotational symmetry class
Triclinic	\emptyset .	0	$\mathbf{I}, \{Z_3\}$
Monoclinic	$\{\mathcal{P}_h\}$	1	$\{Z_2\}, \{Z_4\}, \{SO(2)\}$
Orthotropic	$\{\mathcal{P}_{hv_2}\}$	3	$\{D_2\}, \{T\}$
Trigonal	$\{\mathcal{P}_{v_3}\}$	3	$\{D_3\}$
Tetragonal	$\{\mathcal{P}_{hv_4}\}$	5	$\{D_4\}$
Trans. isotropic	$\{\mathcal{P}_{hv_\infty}\}$	$\infty + 1$	$\{O(2)\}$
Cubic	$\{\mathcal{P}_{\mathcal{O}}\}$	9	$\{\mathcal{O}\}$
Isotropic	$\{\mathcal{P}_{O(3)}\}$	∞^3	$\{SO(3)\}$

the graphic approach of Francois *et al.*⁴⁵ to being able to identify not only the reflection symmetry of a given flexoelectric tensor but also its rotational symmetry.

Let $\mathbf{n} \in S^2$ be the unit vector relative to the reflection transformation $\mathbf{P}(\mathbf{n}) = \mathbf{I} - 2\mathbf{n} \otimes \mathbf{n}$ through the plane $\mathcal{P}(\mathbf{n})$. With no loss of generality, \mathbf{n} is expressed by

$$\mathbf{n} = \sin \theta \cos \phi \mathbf{e}_1 + \sin \theta \sin \phi \mathbf{e}_2 + \cos \theta \mathbf{e}_3 \quad (51)$$

where $(\phi, \theta) \in [0, 2\pi[\times [0, \pi[$ denote, respectively, the longitude and colatitude angles relative to a system of spherical coordinates. Then, by considering, for a given flexoelectric tensor $\mathbb{F} \in \mathcal{F}$, the function:

$$L(\theta, \phi) = \|\mathbf{P}(\theta, \phi) * \mathbb{F} - \mathbb{F}\| = \|\mathbf{P}(\theta, \phi) \cdot \tilde{\mathbf{F}} \cdot \tilde{\mathbf{P}}(\theta, \phi) - \tilde{\mathbf{F}}\| \quad (52)$$

in which $\|\cdot\|$ is the Frobenius norm inherited from the scalar product on \mathcal{F} , $\mathbf{P}(\theta, \phi)$ is a reflection operator parametrized with the longitude and colatitude angles and $\tilde{\mathbf{P}}(\theta, \phi)$ is a 18×18 matrix whose components are obtained by replacing \mathbf{Q} with \mathbf{P} in (23). Finally, the vanishing loci of $L(\theta, \phi)$ give the unit normals to the symmetry planes that \mathbb{F} has.

Concretely, the function (52) is numerically evaluated in a discrete way. Precisely, we introduce

$$M_{ij} = L(\theta_i, \phi_j) \quad \text{with} \quad \theta_i = i \frac{2\pi}{N} \quad \text{and} \quad \phi_j = j \frac{2\pi}{N}$$

where the number N depends on the degree of numerical accuracy required. In our computations, N is set to be equal to 160. To evaluate the function $L(\theta, \phi)$, we first use the matrix representations of flexoelectric tensors presented in Section IV. In addition, the numerical values of the components of a flexoelectric tensor are determined as random integers picked-up in the range $\{-10, 10\}$. We show, in Figure 1, the loci of the zeros of $L(\theta, \phi)$ plotted on the $\theta - \phi$ plane for all rotation symmetry classes and all reflection symmetry classes. It can be seen from Figure 1 that the number of symmetry planes for a given rotation symmetry class or reflection symmetry class coincides exactly with the one provided in Table VI. This also constitutes a validity verification of our theoretical results.

In addition, it can be observed from Figure 1 that, even through the flexoelectric tensors belonging to both rotational symmetry classes $\{Z_3\}$ and \mathbf{I} do not exhibit any reflection symmetry plane, we can differentiate them since the loci of the function $L(\theta, \phi)$ for the flexoelectric tensors belonging to $\{Z_3\}$ are periodic in the ϕ -direction with period $2\pi/3$ while the ones for the flexoelectric tensors appertaining to \mathbf{I} are not periodic. Similarly, even if the flexoelectric tensors belonging to the rotational symmetry classes $\{D_2\}$ and \mathcal{T} possess the same number of reflection symmetry planes, the loci of the function $L(\theta, \phi)$ for flexoelectric tensors belonging to $\{\mathcal{T}\}$ are periodic in the ϕ -direction with period $\pi/2$ but the counterpart of the flexoelectric tensors appertaining to $\{D_2\}$ are periodic in ϕ -direction with period π .

The foregoing graphical approach is now applied to a given flexoelectric tensor $\mathbb{F} \in \mathcal{F}$ with a given angle $\psi \in [0; 2\pi[$ for identifying all invariant directions defined by $\mathbf{n} = \sin \theta \cos \phi \mathbf{e}_1 + \sin \theta \sin \phi \mathbf{e}_2 + \cos \theta \mathbf{e}_3$ in the sense that \mathbb{F} is unchangeable under the rotational transformation action $\mathbf{Q}(\mathbf{n}, \psi)$. As before, by using the well-known Rodrigues expression of $\mathbf{Q}(\mathbf{n}, \psi)$, i.e.

$$\mathbf{Q}(\mathbf{n}, \psi) = \cos(\psi)\mathbf{I} - \sin(\psi)\epsilon \cdot \mathbf{n} + [1 - \cos(\psi)]\mathbf{n} \otimes \mathbf{n} \quad (53)$$

in which ϵ denotes the Levi-Civita third-order tensor, and by introducing the following function

$$J(\theta, \phi, \psi) = \|\mathbf{Q}(\theta, \phi, \psi) * \mathbb{F} - \mathbb{F}\| = \|\mathbf{Q}(\theta, \phi, \psi) \cdot \tilde{\mathbf{F}} \cdot \tilde{\mathbf{Q}}(\theta, \phi, \psi) - \tilde{\mathbf{F}}\| \quad (54)$$

where $\mathbf{Q}(\theta, \phi, \psi)$ is a rotation operator parametrized with the longitude, colatitude and rotation angles; $\tilde{\mathbf{Q}}(\theta, \phi, \psi)$ is a 18×18 matrix whose components are defined by (23), the vanishing loci of $J(\theta, \phi, \psi)$ allow us to obtain the invariant directions \mathbf{n} that \mathbb{F} possesses.

We illustrate, in Figure 2, the vanishing loci of the function $J(\theta, \phi, 2\pi/3)$ plotted on the $\theta - \phi$ plane for a flexoelectric tensor \mathbb{F} belonging to the rotational symmetry class $\{Z_3\}$ whose matrix representation is provided in Section IV. It can be seen from Figure 2 that there exists only one invariant axis spanned by $\mathbf{n} = \mathbf{e}_3$ or $\mathbf{n} = -\mathbf{e}_3$. This is in agreement with the fact that the rotational symmetry class $\{Z_3\}$ contains $\mathbf{Q}(\mathbf{e}_3, 2\pi/3)$.

By combining the knowledge of the matrix representations of all rotational symmetry classes with pole figures, we can finally identify the rotational symmetry class to which a given flexoelectric tensor belongs. The corresponding identification procedure is summarized in Figure 3.

VII. CONCLUDING REMARKS

Flexoelectricity is an electromechanical phenomenon which has a great number of potential applications including energy harvesting, sensors, actuators and biotechnology. A full understanding of the fourth-order flexoelectric tensor is essential not only to the fundamental theory of flexoelectricity but also to all possible applications of flexoelectricity. In the present work, which may be viewed as a continuation of our previous one³⁹, compact explicit matrix representations of the flexoelectric tensor have been provided for all the 12 possible rotational symmetry classes, so as to facilitate its use in various situations; the reflection symmetry classes of the flexoelectric tensor have been also determined and shown to be identical to those of the fourth-order elastic tensor; a simple and efficient graphic method for identifying the rotational symmetry and reflection symmetry of a given flexoelectric tensor has been elaborated and illustrated. These results contribute to developing the continuum theory of flexoelectricity and rendering the use of this theory easier in various anisotropic cases.

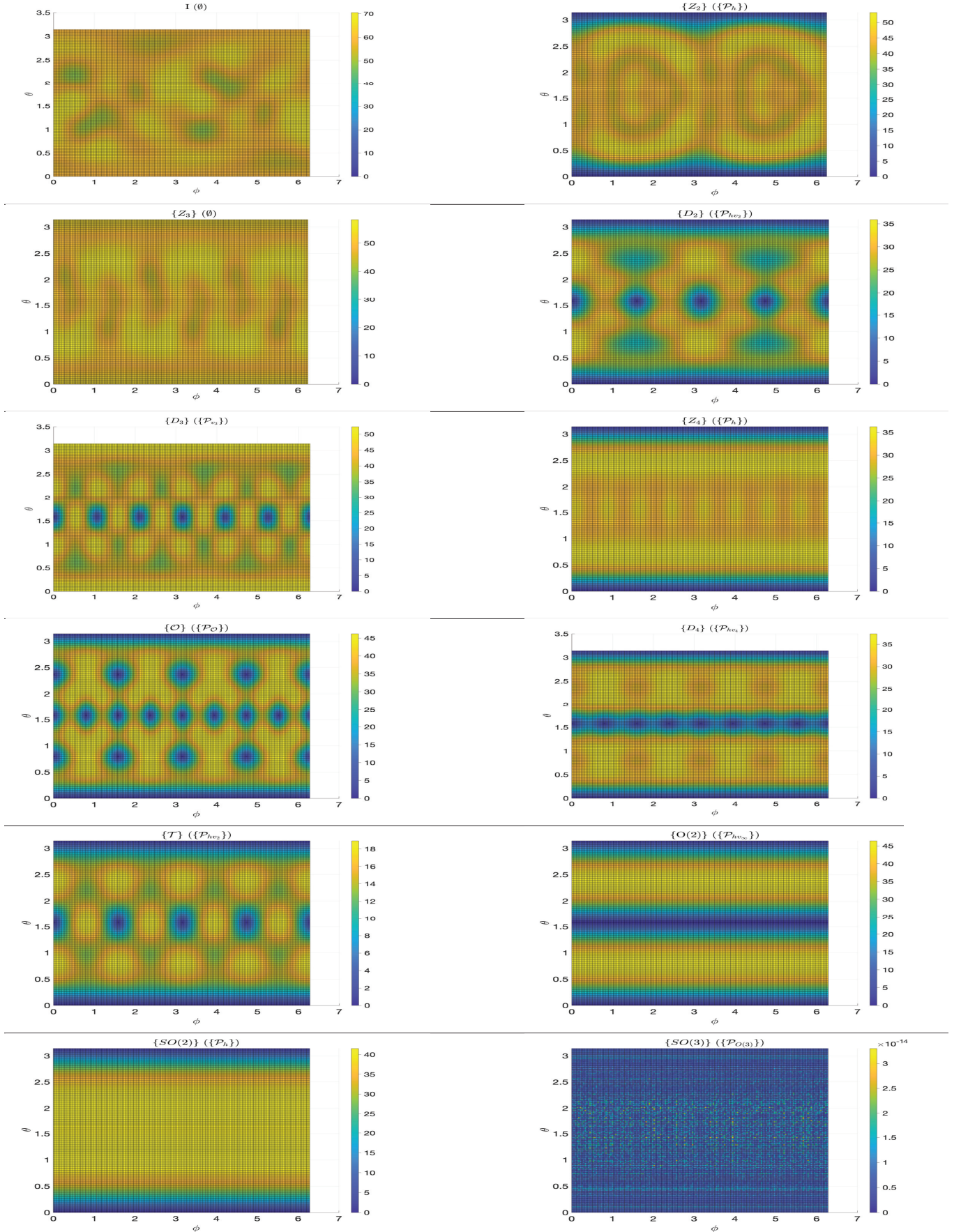


FIG. 1. Loci of the zeros of the function $L(\theta, \phi)$ plotted on the $\theta - \phi$ plane for all rotation symmetry classes and all reflection symmetry classes.

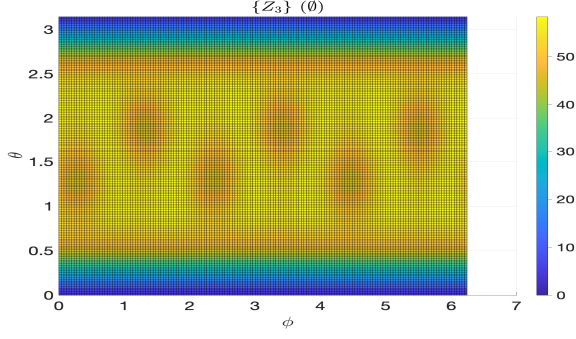


FIG. 2. Loci of the function $J(\theta, \phi, 2\pi/3)$ plotted on the $\theta - \phi$ plane for a flexoelectric tensor \mathbb{F} belonging to the rotational symmetry class $\{Z_3\}$

$$\tilde{\mathbf{F}}_{\text{ABO}_3} = \begin{bmatrix} F_{1111} & F_{2112} & F_{2121} & F_{2112} & F_{2121} & 0 & 0 & 0 & 0 & 0 & 0 & 0 & 0 & 0 & 0 & 0 & 0 & 0 \\ 0 & 0 & 0 & 0 & 0 & F_{1111} & F_{2112} & F_{2121} & F_{2112} & F_{2121} & 0 & 0 & 0 & 0 & 0 & 0 & 0 & 0 \\ 0 & 0 & 0 & 0 & 0 & 0 & 0 & F_{1111} & F_{2112} & F_{2121} & F_{2112} & F_{2121} & F_{2112} & F_{2121} & 0 & 0 & 0 & 0 \end{bmatrix}.$$

The matrix $\tilde{\mathbf{F}}_{\text{ABO}_3}$ has 3 independent components, i.e., the longitudinal flexoelectric coefficient F_{1111} , transverse flexoelectric coefficient F_{2112} and shear flexoelectric coefficient F_{2121} . The values of F_{1111} , F_{2112} and F_{2121} determined experimentally and computationally can be found in Wang *et al.*³⁴ and Shu *et al.*³⁷ for some Pervoskites.

In parallel with the formulation used in the present work in which the electric polarization vector \mathbf{p} is linearly related to the strain gradient \mathbb{E} through the fourth-order flexoelectric tensor \mathbb{F} , there is another formulation of the electric polarization vector \mathbf{p} linearly connected to the second-order derivative of the displacement vector, $\mathbb{U} = \nabla\nabla\mathbf{u}$, as follows (see e.g. Hong *et al.*²⁷):

$$p_i = F_{ijkl}^I U_{jkl} \quad \text{or} \quad p_i = F_{ijkl}^I u_{j,kl}. \quad (55)$$

Here F_{ijkl}^I , the tensor component of the type-I flexoelectric tensor \mathbb{F}^I , possesses the index permutation symmetry $F_{ijkl}^I = F_{ijlk}^I$. Compared with \mathbb{F} , called also type-II flexoelectric tensor, more suitable not only for formulating the thermodynamic theory of ferroelectric materials but also for making comparisons with experimental measurements, the definition of the type-I flexoelectric tensor \mathbb{F}^I is complicated for mathematical derivations of the microscopic theory of flexoelectricity. It can be shown that the connections between \mathbb{F}^I and \mathbb{F} are given by

$$F_{ijkl}^I = \frac{1}{2}(F_{ijkl} + F_{ijlk}), \quad F_{ijkl} = F_{ijkl}^I + F_{ikjl}^I - F_{iljk}^I. \quad (56)$$

In addition, due to the fact that both flexoelectric tensors \mathbb{F}^I and \mathbb{F} exhibit mathematically the same permutation symmetry with respect to two indexes, the flexoelectric tensors \mathbb{F}^I and \mathbb{F} will possess the same rotation and reflection symmetry classifications. Moreover, by adopting

As a simple example of application of our results, we consider Pervoskites with general chemical formula ABO_3 , which are known as ferroelectric materials exhibiting higher permittivity ferroelectrics like flexoelectricity, piezoelectricity and pyroelectricity than the ones of usual dielectric materials, and which are now widely used for the production of electronic components and microtransducers. Since the oxygen octahedral structure of Pervoskites, the symmetry behavior of the corresponding flexoelectricity tensor is cubic and characterized by the rotation symmetry class $\{O\}$ or by the reflection symmetry class $\{P_O\}$. The matrix of the flexoelectricity tensor relative to an appropriate basis, denoted by $\tilde{\mathbf{F}}_{\text{ABO}_3}$, is given by

TABLE VII. Suffix notation correspondences between (j, k, l) and γ .

(j, k, l)	γ
(1,1,1)	1
(1,2,2)	2
(2,1,2) or (2,,2,1)	3
(1,3,3)	4
(3,1,3) or (3,3,1)	5
(2,2,2)	6
(2,1,1)	7
(1,1,2) or (1,2,1)	8
(2,3,3)	9
(3,2,3) or (3,3,2)	10
(3,3,3)	11
(3,1,1)	12
(1,1,3) or (1,3,1)	13
(3,2,2)	14
(2,2,3) or (2,3,2)	15
(3,1,2) or (3,2,1)	16
(2,1,3) or (2,3,1)	17
(1,2,3) or (1,3,2)	18

the reduced suffix notations described in Table VII the fourth-order flexoelectric tensor \mathbb{F}^I with component F_{ijkl}^I can be expressed in a 3×18 matrix form $\tilde{\mathbf{F}}^I$ with components $\tilde{F}_{i\gamma}^I$. Consequently, the number of independent material parameters and compact explicit matrix expression for each of the 12 symmetry classes of flexoelectric tensors \mathbb{F}^I are exactly identical to the ones of \mathbb{F} .

Finally, it is interesting and important to remark that the methods and results presented in the present work are directly applicable to the fourth-order flexomagnetic tensor⁴⁶.

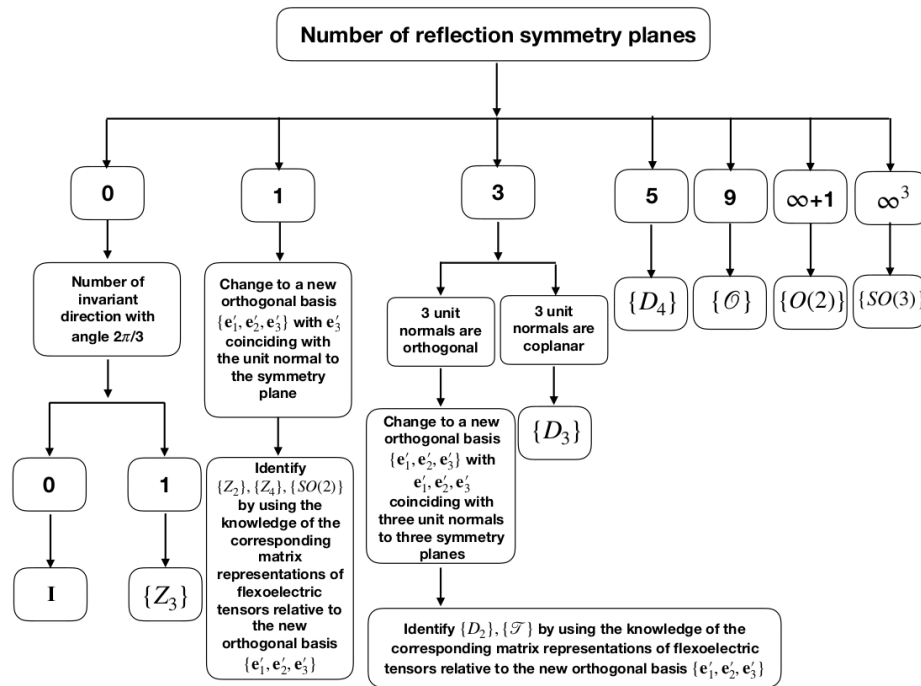


FIG. 3. Procedure for identifying the rotational symmetry class to which a flexoelectric tensor belongs with respect to a given basis

DATA AVAILABILITY

The data that support the findings of this study are available from the corresponding author upon reasonable request.

REFERENCES

- ¹E. V. Bursian and N. N. Trunov (1974). “Nonlocal piezoelectric effect,” *Fiz. Tverd. Tela (Leningrad)*, 16, 1187.
- ²C. Liu, S. Hu and S. Shen (2012). “Effect of flexoelectricity on electrostatic potential in a bent piezoelectric nanowire,” *Smart Mater. Struct.* 21, 115024, Dataset. <https://doi.org/10.1088/0964-1726/21/11/115024>.
- ³T. D. Nguyen, S. Mao, Y.-W. Yeh, P. K. Purohit and M. C. McAlpine (2013). “Nanoscale flexoelectricity,” *Adv. Mater.* 25, 946, Dataset. <https://doi.org/10.1002/adma.201203852>.
- ⁴Z. Yan and L. Y. Jiang (2013). “Flexoelectric effect on the electroelastic responses of bending piezoelectric nanobeams,” *J. Appl. Phys.* 113, 194103, Dataset. <https://doi.org/10.1063/1.4804949>.
- ⁵G. Catalan, L. J. Sinnamon and J. M. Gregg (2004). “The effect of flexoelectricity on the dielectric properties of inhomogeneously strained ferroelectric thin films,” *J. Phys. Condens. Matter.* 16, 2253, Dataset. <https://doi.org/10.1088/0953-8984/16/13/006>.
- ⁶R. B. Meyer (1969). “Piezoelectric effects in liquid crystals,” *Phys. Rev. Lett.* 22, 918, Dataset. <https://doi.org/10.1103/PhysRevLett.22.918>.
- ⁷M. Marvan and A. Havranek (1988). “Flexoelectric effect in elastomers,” *Prog. Colloid. Polym. Sci.* 78, 33, Dataset. <https://doi.org/10.1007/BFb0114342>.
- ⁸W. Ma and L. E. Cross (2001). “Observation of the flexoelectric effect in relaxor $\text{Pb}(\text{Mg}_{1/3}\text{Nb}_{2/3})\text{O}_3$ ceramics,” *Appl. Phys. Lett.* 78, 2920, Dataset. <https://doi.org/10.1063/1.1356444>.
- ⁹W. Ma and L. E. Cross (2002). “Flexoelectric polarization of barium strontium titanate in the paraelectric state,” *Appl. Phys. Lett.* 81, 3440, Dataset. <https://doi.org/10.1063/1.1518559>.
- ¹⁰W. Ma and L. E. Cross (2006). “Flexoelectricity of barium titanate,” *Appl. Phys. Lett.* 88, 232902, Dataset. <https://doi.org/10.1063/1.2211309>.
- ¹¹P. Zubko, G. Catalan, P. R. L. Welche, A. Buckley and J. F. Scott (2007). “Strain-gradient-induced polarization in SrTiO_3 single crystals,” *Phys. Rev. Lett.* 99, 167601, Dataset. <https://doi.org/10.1103/PhysRevLett.99.167601>.
- ¹²S. V. Kalinin and V. Meunier (2008). “Electronic flexoelectricity in low-dimensional systems,” *Phys. Rev. B* 77, 033403, Dataset. <https://doi.org/10.1103/PhysRevB.77.033403>.
- ¹³I. Naumov, A. M. Bratkovsky and V. Ranjan (2009). “Unusual flexoelectric effect in two-dimensional noncentrosymmetric sp^2 -bonded crystals,” *Phys. Rev. Lett.* 102, 217601, Dataset. <https://doi.org/10.1103/PhysRevLett.102.217601>.
- ¹⁴S. Zhang, X. Liang, M. Xu, B. Feng and S. Shen (2015). “Shear flexoelectric response along 3121 direction in polyvinylidene fluoride,” *Appl. Phys. Lett.* 107, 142902, Dataset. <https://doi.org/10.1063/1.4932523>.
- ¹⁵S. Zhang, K. Liu, M. Xu, H. Shen, K. Chen B. Feng and S. Shen (2017). “Investigation of the 2312 flexoelectric coefficient component of polyvinylidene fluoride: Deduction, simulation, and mensuration,” *Sci. Rep.* 7, 3134, Dataset. <https://doi.org/10.1038/s41598-017-03403-7>.
- ¹⁶B. Chu and D.R. Salem (2012). “Flexoelectricity in several thermoplastic and thermosetting polymers,” *Appl. Phys.* 101, 103905, Dataset. <https://doi.org/10.1109/TDEI.2017.006273>.
- ¹⁷Y. Zhou, J. Liu and X.P. Hu (2017). “Flexoelectric effect in PVDF-based polymers,” *IEEE Trans. Dielect. El.* 24, 727, Dataset. <https://doi.org/10.1109/TDEI.2017.006273>.
- ¹⁸E. Sahin and S. Dost (1998). “A strain-gradients theory of elastic dielectrics with spatial dispersion,” *Int. J. Eng. Sci.* 26, 1231.

- Dataset. [https://doi.org/10.1016/0020-7225\(88\)90043-2](https://doi.org/10.1016/0020-7225(88)90043-2).
- ¹⁹A. K. Tagantsev (1986). "Piezoelectricity and flexoelectricity in crystalline dielectrics," *Phys. Rev. B* 34. 5883. Dataset. <https://doi.org/10.1103/PhysRevB.34.5883>.
 - ²⁰A. K. Tagantsev (1991). "Electric polarization in crystals and its response to thermal and elastic perturbation," *Phase Transit.* 35. 119. Dataset. <https://doi.org/10.1080/01411599108213201>.
 - ²¹A. S. Yurkov and A. K. Tagantsev (2016). "Strong surface effect on direct bulk flexoelectric response in solids," *Appl. Phys. Lett.* 108. 022904, Dataset. <https://doi.org/10.1063/1.4939975>
 - ²²B. He, B. Javvaji and X.Y. Zhuang (2018). "Size dependent flexoelectric and mechanical properties of barium titanate nanobelt: A molecular dynamics study," *Physica B.* 545. 527, Dataset. <https://doi.org/10.1016/j.physb.2018.01.031>
 - ²³L. Qi, S.J. Zhou and A.Q. Li (2016). "Size-dependent bending of an electro-elastic bilayer nanobeam due to flexoelectricity and strain gradient elastic effect," *Compos. Struct.* 135. 167, Dataset. <https://doi.org/10.1016/j.compstruct.2015.09.020>
 - ²⁴G. Bai, K. Qin, Q.Y. Xie, X. Yan, C. Gao and Z. Liu (2017). "Size dependent flexocaloric effect of paraelectric Ba_{0.67}Sr_{0.33}TiO₃ nanostructures," *Mater. Lett.* 186. 146, Dataset. <https://doi.org/10.1016/j.matlet.2016.10.001>
 - ²⁵R. Maranganti and P. Sharma (2009). "Atomistic determination of flexoelectric properties of crystalline dielectrics," *Phys. Rev. B* 80. 054109. Dataset. <https://doi.org/10.1103/PhysRevB.80.054109>.
 - ²⁶J.W. Hong and D. Vanderbilt (2011). "First-principles theory of frozen-ion flexoelectricity," *Phys. Rev. B* 84. 180101, Dataset. <https://doi.org/10.1103/PhysRevB.84.180101>
 - ²⁷J.W. Hong and D. Vanderbilt (2013). "First-principles theory and calculation of flexoelectricity," *Phys. Rev. B* 88. 174107, Dataset. <https://doi.org/10.1103/PhysRevB.88.174107>
 - ²⁸F. Deng, Q. Deng and S.P. Shen (2018). "A three-dimensional mixed finite element for flexoelectricity," *J. Appl. Mech.* 85. 031009, Dataset. <https://doi.org/10.1115/1.4038919>
 - ²⁹J. Yvonnet, X. Chen and P. Sharma (2020). "Apparent flexoelectricity due to heterogeneous piezoelectricity," *J. Appl. Mech.* 87. 111003. Dataset. <https://doi.org/10.1115/1.4047981>.
 - ³⁰Q. Li, C.T. Nelson, S.-L. Hsu, A.R. Damodaran, L.-L. Li, A.K. Yadav, M. McCarter, L.W. Martin, R. Ramesh and S.V. Kalinin (2017) "Quantification of flexoelectricity in PbTiO₃/SrTiO₃ superlattice polar vortices using machine learning and phase-field modeling," *Nat. Commun.* 8. 1468, Dataset. <https://doi.org/10.1038/s41467-017-01733-8>
 - ³¹Y.-J. Wang, J. Li, Y.-L. Zhu and X.-L. Ma (2017). "Phase-field modeling and electronic structural analysis of flexoelectric effect at 180° domain walls in ferroelectric PbTiO₃," *J. Appl. Phys.* 122. 224101, Dataset. <https://doi.org/10.1063/1.5017219>
 - ³²N. D. Sharma, R. Maranganti and P. Sharma (2007). "On the possibility of piezoelectric nanocomposites without using piezoelectric materials," *J. Mech. Phys. Solids* 55. 2328. Dataset. <https://doi.org/10.1016/j.jmps.2007.03.016>.
 - ³³P. Zubko, G. Catalan and A. K. Tagantsev (2013). "Flexoelectric effect in solids," *Annu. Rev. Mater. Res.* 43. 387. Dataset. <https://doi.org/10.1146/annurev-matsci-071312-121634>.
 - ³⁴B. Wang, Y. Gu, S. Zhang and L.-Q. Chen (2019). "Flexoelectricity in solids: Progress, challenges, and perspectives," *Prog. Mater. Sci.* 106. 100570. Dataset. <https://doi.org/10.1016/j.pmatsci.2019.05.003>.
 - ³⁵J. Narvaez, F. Vasquez-Sancho and G. Catalan (2016). "Enhanced flexoelectric-like response in oxide semiconductors," *Nature* 538. 219, Dataset. <https://doi.org/10.1038/nature19761>
 - ³⁶A. Abdollahi, F. Vasquez-Sancho and G. Catalan (2018). "Piezoelectric Mimicry of Flexoelectricity," *Phys. Rev. Lett.* 121. 205502, Dataset. <https://doi.org/10.1103/PhysRevLett.121.205502>
 - ³⁷L. Shu, R. Liang, Z. Rao, L. Fei, S. Ke and Y. Wang (2019). "Flexoelectric materials and their related applications: A focused review," *J. Adv. Ceram.* 8. 153, Dataset. <https://doi.org/10.1007/s40145-018-0311-3>
 - ³⁸L. Shu, S. Ke, L. Fei, W. Huang, Z. Wang, J. Gong, X. Jiang, L. Wang, F. Li, S. Lei, Z. Rao, Y. Zhou, R.-K. Zheng, X. Yao, Y. Wang, M. Stengel and G. Catalan (2020). "Photoflexoelectric effect in halide perovskites," *Nat. Mater.* 19. 605, Dataset. <https://doi.org/10.1038/s41563-020-0659-y>
 - ³⁹H. Le Quang and Q.-C. He (2011). "The number and types of all possible rotational symmetries for flexoelectric tensors," *Roy. Soc. London, Ser. A* 467. 2369. Dataset. <https://doi.org/10.1098/rspa.2010.0521>.
 - ⁴⁰L. Shu, X. Wei, T. Pang, X. Yao and C. Wang (2011). "Symmetry of flexoelectric coefficients in crystalline medium," *J. Appl. Phys.* 110. 104106. Dataset. <https://doi.org/10.1063/1.3662196>.
 - ⁴¹A. Spencer (1970). "A note on the decomposition of tensors into traceless symmetric tensors," *Int. J. Engng. Sci.* 8. 475. Dataset. [https://doi.org/10.1016/0020-7225\(70\)90024-8](https://doi.org/10.1016/0020-7225(70)90024-8).
 - ⁴²S. Forte and M. Vianello (1996). "Symmetry classes for elasticity tensors," *J. Elasticity* 43. 81. Dataset. <https://doi.org/10.1007/BF00042505>.
 - ⁴³S. Forte and M. Vianello (1997). "Symmetry classes and harmonic decomposition for photoelasticity tensors," *Int. J. Engng. Sci.* 14. 1317. Dataset. [https://doi.org/10.1016/S0020-7225\(97\)00036-0](https://doi.org/10.1016/S0020-7225(97)00036-0).
 - ⁴⁴P. Chadwick, M. Vianello and S. Cowin (2001). "A new proof that the number of linear anisotropic elastic symmetries is eight," *J. Mech. Phys. Solids* 49. 2471. Dataset. [https://doi.org/10.1016/S0022-5096\(01\)00064-3](https://doi.org/10.1016/S0022-5096(01)00064-3).
 - ⁴⁵M. Francois, G. Geymonat and Y. Berthaud (1998). "Determination of the symmetries of an experimentally determined stiffness tensor: Application to acoustic measurements," *Int. J. Solids Struct.* 35. 4091. Dataset. [https://doi.org/10.1016/S0020-7683\(97\)00303-x](https://doi.org/10.1016/S0020-7683(97)00303-x).
 - ⁴⁶P. Lukashev and R. F. Sabirianov (2010). "Flexomagnetic effect in frustrated triangular magnetic structures," *Phys. Rev. B* 82. 094417. Dataset. <https://doi.org/10.1103/PhysRevB.82.094417>.